DALTON
FULL PAPER

The synthesis, structure, magnetic and Mössbauer spectral properties of an Fe–Zr carboxylate–alkoxide derivative containing an $\{Fe_2Zr_2(\mu_3\text{-}O)_2\}$ core

Paul S. Ammala,[a] John D. Cashion,[b] Christopher M. Kepert,[a] Keith S. Murray,[a] Boujemaa Moubaraki,[a] Leone Spiccia[a] and Bruce O. West*[a]

[a] *School of Chemistry, PO Box 23, Monash University, Victoria, Australia 3800. E-mail: bruce.west@sci.monash.edu.au*
[b] *School of Physics and Materials Engineering, PO Box 27, Monash University, Victoria, Australia 3800*

Received 15th February 2001, Accepted 15th May 2001
First published as an Advance Article on the web 14th June 2001

Reaction of $[Fe_3(\mu_3\text{-}O)(O_2CPh)_6(H_2O)_3](O_2CPh)$ with pyridine yields a product (**2**) which on recrystallisation rearranges to $[Fe_6(\mu\text{-}O)_2(\mu\text{-}OH)_2(O_2CPh)_{12}(py)_2]$ (**3**). Magnetic and Mössbauer spectral analyses suggest that compound (**2**) contains an $Fe_4(O)_2$ cluster. The unrecrystallised material (**2**) reacts with $Zr(OBu^t)_4$ to form $[Fe_2Zr_2(\mu_3\text{-}O)_2(\mu\text{-}O_2CPh)_6(OBu^t)_4(py)_2]$ (**4**). The mixed metal cluster has a "butterfly" configuration with Fe^{III} atoms coordinated by pyridine forming the "body" position. It displays weak antiferromagnetic behaviour, closely modelled as an Fe_2O_2 dimer with $g = 2.01$ and $J = -1.42$ cm^{-1}. Its Mössbauer spectrum has the high-spin Fe(III) parameters $\delta = 0.51$ mm s^{-1} and $\Delta E_Q = 0.65$ mm s^{-1} at 5 K. The molecular species $[Zr_3(\mu_3\text{-}O)(\mu\text{-}O_2CPh)_2(\mu\text{-}OBu^t)_2(OBu^t)_6]$ (**5**) is also detected in the reaction when excess $Zr(OBu^t)_4$ is present.

Introduction

A number of mixed metal complexes has been prepared and characterised by the reaction between a metal alkoxide and a second metal compound such as a halide, a chelate complex, *e.g.* an acetylacetonate, or a carboxylate.[1] Such complexes have proved useful in themselves or have been shown to be implicated in hydrolytic, so called "sol–gel processes", to produce mixed metal oxides having important electronic properties. Several commercially significant oxides having the perovskite structure have proved to be readily formed with the aid of such complexes.[2]

Fe^{III}–Zr alkoxide complexes are of interest because of their potential use to add small amounts of Fe^{III} to zirconia produced by the sol–gel process. The presence of Fe^{III} ions in the ZrO_2 lattice can influence the crystal form of the final oxide, particularly favoring formation of the technically useful cubic phase.[3,4] A sol–gel procedure for the preparation of zirconia involving hydrolysis of a $Zr(OR)_4$ compound in alcohol solution in the presence of $Fe(acac)_3$ with subsequent heating of the gel so formed[5,6] has been described. An Fe–Zr complex, $[Zr_3Fe(\mu_4\text{-}O)(\mu_2\text{-}OPr^n)_6(OPr^n)_4(acac)_3]$, formed by reaction between $Zr(OPr^n)_4$ and $Fe(acac)_3$ has been structurally characterised.[7] Another Fe–Zr compound[8] prepared by the interaction of $FeCl_3$ with $K[Zr_2(OPr^i)_9]$ has been allocated the empirical formula $Fe^{III}[Zr_2(OPr^i)_9]_3$ although a structural study has not yet been reported. However there are disadvantages to the use of such complexes in sol–gel procedures. Thus, high temperatures would be necessary to ensure total elimination of acetylacetonate residues which are not readily removed by hydrolysis[9] while it is difficult to ensure complete removal of deleterious halide impurities from the final oxide. There would, therefore, be benefits in using complexes formed by interaction between carboxylates and alkoxides. The final oxide formed by hydrolysis of compounds containing such ligands will be free of both ligands after a combination of hydrolysis and heating at relatively low temperatures.

A potential route for the preparation of an Fe–Zr alkoxide precursor compound would be to react an oxo bridged, "basic" Fe^{III} carboxylate, $[Fe_3(\mu_3\text{-}O)(O_2CR)_6(L)_3]X$,[10] with a Zr alkoxide in an appropriate solvent. There are however certain restrictions on choice of solvent when designing a synthetic procedure for the preparation of an Fe–Zr complex from such reagents. Although alcohols have been extensively used as the solvent media for sol–gel processes they are predictably less useful in synthetic studies involving "basic" Fe^{III} carboxylates since reactions are known to occur readily between the alcohol and Fe^{III} salt. For example, an early report showed that $[Fe_3(\mu_3\text{-}O)(O_2CCH_3)_6(H_2O)_3](ClO_4)$ reacts with methanol to give an Fe^{III} alkoxo–carboxylato complex[11] product. It was not possible to structurally characterise this complex, but it showed the magnetic and Mössbauer spectral properties of a tetranuclear compound. More recent studies involving successful structural characterisations have shown that reactions involving $[Fe_3(\mu_3\text{-}O)(O_2CR)_6(H_2O)_3]X$ salts and alcohols yield decameric $[Fe(O_2CR)(OR')_2]_{10}$ compounds[12,13] while an octanuclear species $[Fe_8(\mu_3\text{-}O)_2(\mu_4\text{-}O)_2(O_2CPh)_{14}(OCH_2Bu^t)_2(HOCH_2Bu^t)_2]$[14] results from the reaction of neopentanol and $[Fe_3(\mu_3\text{-}O)(O_2CPh)_6(H_2O)_3](O_2CPh)$.

Non-coordinating solvents such as benzene or toluene would be more suitable choices for mixed metal complex syntheses. However the compound $[Fe_3(\mu_3\text{-}O)(O_2CPh)_6(H_2O)_3](O_2CPh)$,[15] although soluble in toluene suffered the disadvantage that the labile water molecules coordinated to the metal centres caused hydrolysis of metal alkoxide linkages. The nitrate salt of the pyridine substituted cation, $[Fe_3(\mu_3\text{-}O)(O_2CPh)_6(py)_3](NO_3)$, has been structurally defined[16a] but its insolubility in benzene or toluene, as is generally true for "basic" Fe^{III} carboxylates having inorganic counter anions, did not make it an ideal alternative choice. The toluene solubility of the aqua–benzoate suggested that the benzoate salt of the tris-pyridinate cation might prove a more suitable reagent for reaction with Zr alkoxides and led to the attempts reported in this paper to prepare the previously unknown "basic" Fe^{III} benzoate, $[Fe_3(\mu_3\text{-}O)(O_2CPh)_6(py)_3](O_2CPh)$, from the aqua substituted compound. Although the desired complex was not successfully obtained, the product of the substitution reaction (compound (**2**)) was found a suitable reagent and allowed the isolation of an Fe–Zr complex.

 DOI: 10.1039/b101500l

Magnetic and Mössbauer spectral evidence as to a possible constitution of (**2**) are presented.

Experimental

The alkoxides used and any products containing alkoxide groups were susceptible to hydrolysis in air in both the solid state and in solution. All operations were performed using greaseless Schlenk apparatus and cannulation techniques, under an atmosphere of dry nitrogen. Moisture sensitive solids were stored under nitrogen in Schlenk flasks, or a dry nitrogen glove box. Samples for magnetic moment and Mössbauer spectral measurements were placed in the appropriate containers within the dry box.

Physical measurements

Elemental analyses (CHN) were carried out by National Analytical Laboratories (NAL). Compounds considered to be moisture sensitive were sealed in glass ampoules under nitrogen and analysed by Chemical Microanalytical Services (CMAS). IR spectra were measured on a Perkin-Elmer Series 1640 FTIR spectrophotometer, using liquid paraffin and/or Fluorolube mulls between sodium chloride plates.

Magnetic susceptibilities were obtained over the temperature range 300–2 K using a Quantum Design MPMS 5 SQUID instrument in an applied field of 1.0 Tesla. Samples of mass *ca.* 25 mg, which were stable in air, were contained in a gel capsule held in the centre of a drinking straw fixed to the end of the sample rod. Those samples of compounds which could lose solvent of crystallisation when exposed to air were contained in sealed quartz tubes. The instrument was calibrated against a standard sample of palladium and the chemical calibrants $CuSO_4 \cdot 5H_2O$ and $[Ni(en)_3](S_2O_3)$. Diamagnetic corrections were applied using Pascal's constants.

Mössbauer spectra were recorded using a conventional constant-acceleration drive-system with a symmetrical waveform. The radiation source was ^{57}Co in Rh. Calibration was made with natural α-Fe foil. The source was always at room temperature and isomer shifts given with respect to α-Fe at room temperature. Spectra of complexes examined in this work were fitted using Lorentzian lineshapes unless otherwise described in the text.

Preparation of $[Fe_3(O)(O_2CPh)_6(py)_3](NO_3)$ (1)[16a]

$[Fe_3O(O_2CPh)_6(H_2O)_3](NO_3)$ was prepared by reaction of $Fe(NO_3)_3 \cdot 6H_2O$ with NaO_2CPh in aqueous solution following a general procedure[17,18] and a suspension of the salt in CH_2Cl_2 reacted with pyridine resulting in dissolution of the solid. The addition of diethyl ether then induced precipitation. The brown solid was washed with ether and dried by pumping at 10^{-3} Torr. Yield: 64%. Found: C, 55.4; H, 3.9; N, 5.2%. Calc. for $C_{57}H_{45}N_4O_{16}Fe_3$: C, 56.6; H, 3.75; N, 4.63% (low C values were also previously reported for this compound[16a]).

The reaction of pyridine with $[Fe_3(O)(O_2CPh)_6(H_2O)_3](O_2CPh)$: compound (2)

Pyridine (1.5 ml, 18.5 mmol) was added to a solution of $[Fe_3(O)(O_2CPh)_6(H_2O)_3](O_2CPh)$[18] (1.00 g, 0.9 mmol) in toluene (50 ml) at 90 °C and the resulting solution heated to reduce its volume by one third. The solution was left to cool overnight, protected from ingress of water and green-brown micro-crystals of (**2**) were deposited. These were washed with hot toluene and dried under high vacuum. An alternative preparation in which the aqua salt was first dissolved in pyridine, toluene added and the mixture heated at reflux, also resulted in deposition of the same product on cooling. Repeat preparations by either procedure with small variations in reaction times gave material having similar microanalyses and indicated constant composition. Found: Sample (i) C, 60.8; H, 4.2; N, 2.0%. Sample (ii) C, 60.7; H, 4.1; N, 1.9%. Calc. for $[Fe_3(O)(O_2CPh)_6(py)_2(H_2O)](O_2CPh) \cdot C_6H_5CH_3$ ($C_{66}H_{55}N_2O_{16}Fe_3$) (**2a**): C, 61.0; H, 4.27; N, 2.16%. Calc. for $[Fe_4(O)_2(O_2CPh)_8(C_5H_5N)_2] \cdot 1.5C_6H_5CH_3$ ($C_{75.5}H_{62}N_2O_{18}Fe_4$) (**2b**): C, 60.4; H, 4.11; N, 1.84%. IR (ν/cm^{-1}): (no clearly identifiable OH stretch due to water band); 1605(m), 1560(s), 1542(s), 1518(s), 1492(w), 1398(vs), 1218(m), 1025(m), 716(s).

Yields of (**2**) (0.81–0.97 g) ranging between 72 and 86% calculated on the basis of formula (**2a**) were obtained. Crystals of (**2**) suitable for a single crystal X-ray diffraction study could not be isolated from any of the preparations despite variations in the reaction time and rate of cooling.

The slow evaporation of a CH_2Cl_2–ethyl acetate solution of a sample of (**2**) in air, resulted in the deposition of red crystals which slowly lost their shape when exposed to air over several days, presumably due to loss of solvent. An X-ray structure determination carried out on a crystal obtained directly from the mother liquor identified the product as a solvate of the hexanuclear compound $[Fe_6(O)_2(OH)_2(O_2CPh)_{12}(py)_2] \cdot 2EtO_2CMe \cdot H_2O$ (**3**). (A sample of the material was pumped at 10^{-3} Torr for several hours to remove solvent of crystallisation before microanalysis.) Found: C, 56.7; H, 4.0; N, 1.4%. Calc. for $[Fe_6(O)_2(OH)_2(O_2CPh)_{12}(py)_2]$ ($C_{94}H_{72}N_2O_{28}Fe_6$): C, 56.1; H, 3.61; N, 1.39%. IR (ν/cm^{-1}): 1601(s), 1568(s), 1544(s), 1492(m), 1456(vs), 1415(vs), 1217(m), 1174(m), 1068(m), 718(vs).

Reaction of Fe carboxylates with $Zr(OR)_4$

$[Fe_3O(O_2CPh)_6(py)_3](NO_3)$ (1). This compound is insoluble in benzene or toluene and no dissolution of the compound occurred when up to six equivalents of $Zr(OR)_4$ (R = Pr^n, Pr^i, Bu^n, Bu^t) were added and the mixtures refluxed, indicating that no reaction had occurred. Similarly there was no reaction between the benzene-insoluble $[Fe_3O(O_2CPh)_6(H_2O)_3](NO_3)$ and $Zr(OR)_4$ under similar conditions.

Compound (2). (The formula (**2b**) was used for convenience in calculating quantities.) The typical reaction procedure carried out at room temperature involved adding one, two, three or six equivalents of $Zr(OR)_4$ either directly as a liquid, or a concentrated solution in solvent (2 ml), to a suspension of (**2**) in the same solvent (5 ml). The resulting mixture was then stirred for 24 hours, and any undissolved solid allowed to settle for a further 24 hours before decanting the supernatant solution. The Fe(III) complex showed additional solubility in the presence of $Zr(OR)_4$ (R= Pr^n, Pr^i, Bu^n) in toluene, benzene and diethyl ether, but readily dissolved in CH_2Cl_2 even before addition of $Zr(OR)_4$. Careful evaporation of the solutions resulted in deposition of red, glassy solids rather than crystalline products.

Preparation of $[Fe_2Zr_2O_2(O_2CPh)_6(OBu^t)_4(py)_2] \cdot 2C_6H_6$ (4)

$Zr(OBu^t)_4$ (0.16 g, 0.42 mmol) was added to a suspension of (**2**) (0.18 g, 0.12 mmol calc. as (**2b**)) in benzene (7 ml) causing all but a trace of the Fe complex to have dissolved within 24 hours after addition of the alkoxide. Careful evaporation of the yellow-orange solution under N_2 yielded yellow crystals of (**4**). A crystal suitable for X-ray structural analysis was obtained from the mother liquor. The remaining crystals were isolated and washed with benzene prior to analysis (Yield: 0.14 g, 71%). Found: C, 57.5; H, 5.5; N, 1.6%. Calc. for $C_{68}H_{76}N_2O_{18}Fe_2Zr_2 \cdot 2C_6H_6$: C, 58.0; H, 5.23; N, 1.69%. Electron microprobe analysis gave Fe : Zr, 1 : 1. IR (ν/cm^{-1}): 1607(s), 1569(s), 1545(m), 1527(m), 1492(m), 1417(vs), 1225(w), 1209(m), 1192(m), 1176(m), 1073(w). 1073(m), 1025(s), 995(s), 900(s), 720(s), 673(s).

Reactions between (**2**) and $Zr(OBu^t)_4$ using 1 or 2 equivalents of the alkoxide also resulted in the formation of yellow coloured crystals. Microanalyses, electron microprobe and

Table 1 Summary of crystal data for $[Fe_6(O)_2(OH)_2(O_2CPh)_{12}(py)_2]\cdot 2EtO_2CMe\cdot H_2O$ (**3**), $[Fe_2Zr_2(O)(O_2CPh)_6(OBu^t)_4]\cdot 2C_6H_6$ (**4**) and $[Zr_3(O)(OBu^t)_8(O_2CPh)_2]$ (**5**)

Compound	**3**	**4**	**5**
Empirical formula	$C_{102}H_{90}N_2O_{33}Fe_6$	$C_{80}H_{88}N_2O_{18}Fe_2Zr_2$	$C_{46}H_{82}O_{13}Zr_3$
M	2206.91	1659.71	1116.81
Crystal system	Monoclinic	Monoclinic	Monoclinic
Space group	$P2_1/c$ (no. 14)	$P2_1/n$ (no. 14)	$P2_1/n$ (no. 14)
a/Å	15.5770(3)	21.9474(2)	13.8655(1)
b/Å	24.3839(3)	12.6078(1)	18.2710(2)
c/Å	27.3633(5)	29.5332(1)	21.5606(2)
β/°	103.013(7)	101.9886(6)	93.582(1)
V/Å^3	10126.4(4)	7993.8(1)	5451.42(8)
Z	4	4	4
D_c/g cm^{-3}	1.45	1.38	1.36
μ/cm^{-1}	9.19	6.76	6.17
T/K	123(2)	123(2)	123(2)
2θ range/°	61.0	55.0	60.1
No. collected	25161	19017	16286
No. observed	11720	11162	11540
R	0.078	0.036	0.039
R_w	0.100	0.029	0.042
Largest (smallest) difference peak/e Å^{-3}	4.28 (−1.05)	0.60 (−0.52)	1.86 (−1.86)

infrared spectroscopic examination indicated they consisted of (**4**).

Preparation of $[Zr_3(O)(OBu^t)_8(O_2CPh)_2]$ (5)

The reaction of (**2**) (0.18 g, 0.12 mmol calc. as (**2b**)) with 6 molar equivalents of $Zr(OBu^t)_4$ (0.32 g, 0.83 mmol) in benzene (7 ml), allowed all of the Fe complex to dissolve in the 24 hour period after the addition of $Zr(OBu^t)_4$. Evaporation of the yellow-orange solution under N_2 yielded yellow coloured crystals. A single pale yellow coloured crystal which had grown on the wall of the reaction vessel, separate from the bulk of the crystalline mass of (**4**) at the bottom of the reaction vessel, was chosen for structural characterisation by X-ray diffraction. The material was found to be $[Zr_3(O)(OBu^t)_8(O_2CPh)_2]$ (**5**). Electron microprobe examination of a portion of the crystal showed <1% of Fe was present in the Zr compound. Insufficient material remained for a microanalysis. IR (ν/cm^{-1}): 1601(s), 1557(s), 1539(s), 1494(w), 1416(s), 1230(s), 1201(s), 1026(s), 988(s), 900(s); 718(s).

Structure determinations

X-Ray crystallographic measurements were performed using a Nonius Kappa CCD diffractometer, fitted with a Mo-Kα radiation source and graphite monochromator ($\lambda = 0.71069$). All refinement calculations were performed using the teXsan crystallographic package.[19] In each determination conditions for convergence were met with $R = \Sigma||F_o| - |F_c||/\Sigma|F_o|$ and $R_w = (\Sigma\omega(|F_o| - |F_c|)^2/\Sigma(|F_o|^2)^{1/2}$ while the average standard deviation (goodness of fit value) of an observation of unit weight was given by $(\Sigma\omega(|F_o| - |F_c|)^2/(N_{observns} - N_{params})\}^{1/2})$. Neutral atom scattering factors taken from Cromer and Waber[20] were employed. Non-hydrogen atoms in the structure were refined by full-matrix least-squares by employing anisotropic thermal parameters. Hydrogen atoms were included in the structure, in geometrically idealised positions (C–H = 0.96 Å), but were not included in the refinement. Crystallographic data for the various structure determinations are given in Table 1.

CCDC reference numbers 158771–158773.

See http://www.rsc.org/suppdata/dt/b1/b101500l/ for crystallographic files in CIF or other electronic format.

Results and discussion

Synthesis of Fe^{III} reaction intermediate compound (2)

Neither of the "basic" Fe^{III} carboxylates $[Fe_3(O)(O_2CPh)_6(L)_3](NO_3)$(L = H_2O, py) is soluble in benzene or toluene nor is there any sign of reaction when suspensions of the compounds in those solvents were warmed with a Zr alkoxide. On the other hand, $[Fe_3(O)(O_2CPh)_6(H_2O)_3](O_2CPh)$ is soluble in the warm solvents and it was anticipated that the pyridine substituted analogue $[Fe_3(\mu_3\text{-}O)(O_2CPh)_6(py)_3](O_2CPh)$ would also be soluble and would be the compound of choice for reaction with $Zr(OR)_4$ species. Although this particular benzoate salt has not been reported previously, many other complexes tri-substituted with N-heterocycles have been prepared by the ready replacement of water from the corresponding aqua substituted derivative $[Fe_3(\mu_3\text{-}O)(O_2CR)_6(H_2O)_3]X$ by reaction with a heterocycle such as pyridine, in a suitable solvent.[16,21]

Refluxing a toluene/pyridine solution of $[Fe_3(O)(O_2CPh)_6(H_2O)_3](O_2CPh)$ for a short time resulted in the precipitation of a brown-green coloured product (**2**) which was soluble in warm toluene. However its C, H, N microanalytical data indicated less pyridine to be present than would correspond to the desired product $[Fe_3(O)(O_2CPh)_6(py)_3](O_2CPh)$. The microanalyses of a sample of (**2**) obtained from a repeat preparation gave concordant results supporting the view that the product (**2**) could be reproducibly formed and had a homogeneous composition. An empirical formula for (**2**) initially derived from the analytical data suggested it could be the bis-pyridinated complex $[Fe_3(\mu_3\text{-}O)(O_2CPh)_6(py)_2(H_2O)](O_2CPh)$ (**2a**) solvated by toluene.[14] Such partially substituted M–μ_3-oxo compounds have been characterised for mixed valence Mn compounds *e.g.* $[Mn^{II}Mn^{III}_2(\mu_3\text{-}O)(O_2CR)_6(py)_2(H_2O)]$[22] but only one unsymmetrically substituted $Fe_3(\mu_3\text{-}O)$ carboxylate has been structurally characterised,[23] $[Fe_3(\mu_3\text{-}O)(O_2CPh)_6(CH_3OH)_2(H_2O)](O_2CPh)$. Moreover, pyridine substitution of water in aqua substituted "basic" Fe^{III} carboxylates has been found to be complete in such substitution reactions published hitherto.[16,21] A single crystal of quality suitable for an X-ray structural study could not be isolated from the reaction product as it was first precipitated and recrystallisation of a sample of (**2**) was attempted using a mixed CH_2Cl_2–ethyl acetate solvent in which the product was reasonably soluble. A red crystalline derivative (**3**) was recovered and an X-ray structural study showed it to be the hexanuclear complex $[Fe_6(\mu_3\text{-}O)_2(\mu\text{-}OH)_2(O_2CPh)_{12}(py)_2]\cdot 2EtO_2CMe\cdot H_2O$. The molecule has an $\{Fe_6(\mu_3\text{-}O)_2(OH)_2\}^{12+}$ core similar to that observed in the H_2O–1,4-dioxane coordinated species described earlier.[24] Fig. 1(a) is an ORTEP diagram showing the atom arrangement and Fig. 1(b) shows the twisted boat type configuration of the $\{Fe_6(\mu_3\text{-}O)_2(OH)_2\}^{12+}$ core as was also observed for the H_2O–

Table 2 Selected bond distances (Å) and angles (°) for $[Fe_6(\mu\text{-}O)_2(OH)_2(O_2CPh)_{12}(py)_2]\cdot 2EtO_2CMe\cdot H_2O$ (**3**) (estimated standard deviations given in parentheses)

Fe(1)–O(1)	1.883(6)	Fe(2)–O(1)	1.942(6)
Fe(1)–O(5)	2.041(7)	Fe(2)–O(3)	2.003(6)
Fe(1)–O(7)	2.040(7)	Fe(2)–O(6)	2.010(7)
Fe(1)–O(9)	2.023(7)	Fe(2)–O(8)	2.034(6)
Fe(1)–O(11)	2.023(7)	Fe(2)–O(13)	1.982(6)
Fe(1)–N(1)	2.245(8)	Fe(2)–O(15)	2.045(7)
Fe(3)–O(4)	1.929(6)	Fe(3)–O(1)	1.958(6)
O(1)–Fe(1)–O(5)	99.8(3)	O(1)–Fe(1)–O(7)	97.6(3)
O(1)–Fe(1)–O(9)	97.8(3)	O(1)–Fe(1)–O(11)	93.9(3)
O(1)–Fe(1)–N(1)	176.0(3)	O(5)–Fe(1)–O(7)	86.4(3)
O(5)–Fe(1)–O(9)	88.0(3)	O(5)–Fe(1)–O(11)	166.3(3)
O(5)–Fe(1)–N(1)	84.1(3)	O(7)–Fe(1)–O(9)	164.3(3)
O(7)–Fe(1)–O(11)	90.7(3)	O(7)–Fe(1)–N(1)	83.5(3)
O(9)–Fe(1)–O(11)	91.3(3)	O(9)–Fe(1)–N(1)	81.3(3)
O(11)–Fe(1)–N(1)	82.2(3)		
O(1)–Fe(2)–O(3)	93.3(3)	O(1)–Fe(2)–O(6)	94.5(3)
O(1)–Fe(2)–O(8)	94.5(3)	O(1)–Fe(2)–O(13)	92.8(3)
O(1)–Fe(2)–O(15)	178.6(3)	O(3)–Fe(2)–O(6)	170.5(3)
O(3)–Fe(2)–O(8)	87.2(3)	O(3)–Fe(2)–O(13)	98.9(3)
O(3)–Fe(2)–O(15)	87.6(3)	O(6)–Fe(2)–O(8)	86.8(3)
O(6)–Fe(2)–O(13)	86.1(3)	O(6)–Fe(2)–O(15)	84.4(3)
O(8)–Fe(2)–O(13)	170.2(3)	O(8)–Fe(2)–O(15)	84.6(3)
O(13)–Fe(2)–O(15)	88.0(3)		
Fe(1)–O(1)–Fe(2)	118.8(3)	Fe(1)–O(1)–Fe(3)	119.3(3)
Fe(2)–O(1)–Fe(3)	121.5(3)	Fe(2)–O(3)–Fe(4)	131.0(3)

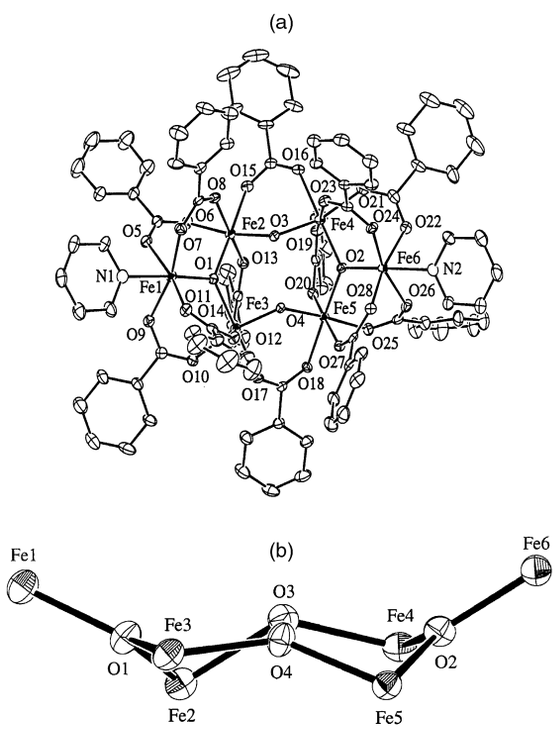

Fig. 1 ORTEP[44] diagrams: (a) $[Fe_6(\mu_3\text{-}O)_2(\mu\text{-}OH)_2(O_2CPh)_{12}(py)_2]\cdot 2EtO_2CMe\cdot H_2O$ (**3**); (b) the $\{Fe_6(\mu_3\text{-}O)_2(\mu\text{-}OH)_2\}^{12+}$ skeletal core.

dioxane coordinated product. Apart from the coordination of pyridine, the general bond distances and angles in (**3**) (Table 2) are quite similar to those reported for the H_2O–dioxane compound. The bridging OH groups lie on the same side of the molecular unit (Fig. 1(b)) with the O(H)–O(H) distance, 2.55 Å, slightly longer than the same distance (2.46 Å) noted for the dioxane derivative. Interestingly, the latter molecule had been formed by recrystallising the tris-aqua complex, $[Fe_3(\mu_3\text{-}O)(O_2CPh)_6(H_2O)_3](O_2CPh)$, from an acetonitrile–dioxane mixture.

Magnetism and Mössbauer spectra of (1), (2) and (3)

In the absence of a structural study the temperature variation of the magnetic susceptibility of (**2**) and its Mössbauer spectrum were examined to provide information as to its likely constitution. The corresponding data for the structurally characterised $[Fe_3(\mu_3\text{-}O)(O_2CPh)_6(py)_3](NO_3)$ (**1**) were obtained for comparison together with that for $[Fe_6(\mu_3\text{-}O)_2(\mu\text{-}OH)_2(O_2CPh)_{12}(py)_2]$ (**3**) as the product obtained on recrystallisation of (**2**).

The plot of magnetic moment *versus* temperature for the tris-pyridine derivative (**1**) displays the characteristic drop with lowering of temperature commensurate with antiferromagnetic behaviour. The magnetic moment at 300 K per Fe atom (μ_{Fe}) is 3.25 μ_B, comparable to the values found for the tri-aqua substituted benzoate and other $\{Fe_3(\mu\text{-}O)\}^{7+}$ compounds. The curve can be readily modelled by the well known procedure developed for such $Fe_3(\mu\text{-}O)$ complexes using a spin Hamiltonian $(-2J\boldsymbol{S}_i\cdot\boldsymbol{S}_j)$ based either on an isosceles or equilateral triangular arrangement of the Fe atoms.[25,26]

As in other cases where crystallographic evidence would also indicate that an equilateral array of metal ions exists in the solid state the isosceles triangular method gave a slightly better fit to the data[18] with $J = -28.2$ cm^{-1}, $J' = -32.6$ cm^{-1} and $g = 2.00$. Further light has been thrown onto this situation by a recent paper[16b] in which an X-ray study of the complex $[Fe_3(O)(O_2CPh)_6(py)_3](ClO_4)\cdot py$ has shown it to have a similar three-fold symmetry to (**1**). It has been further shown by inelastic neutron scattering spectra at 1.5 K to contain two inequivalent molecules. One has a static isosceles triangular structure with $J = -25.6$ cm^{-1} and $J' = -28.5$ cm^{-1} comparable to the values found for (**1**). The other molecular species is a dynamic system with pseudorotation between equivalent isosceles geometries. These J values compare with $J = -29.9$ cm^{-1} and $J' = -44.4$ cm^{-1} for the starting material $[Fe_3(O)(O_2CPh)_6(H_2O)_3](O_2CPh)$ measured in this study. Long *et al.*[18] previously reported $J = -29.6$ cm^{-1} and $J' = -20.2$ cm^{-1} for a water solvate of the aqua benzoate complex.

The $\{Fe_6(\mu_3\text{-}O)_2(\mu\text{-}OH)_2(py)_2\}^{12+}$ complex (**3**) (Fig. 2(b)) also shows antiferromagnetic behaviour. Its magnetic moment per Fe atom at 300 K is comparable to the value of 3.0 μ_B reported for the dioxane–water coordinated analogue.[24] The μ_{eff} values decrease rapidly between 300 and 50 K, then more rapidly, reaching 1.05 μ_B at 4.2 K consistent with an $S = 0$ ground state as was also found for the dioxane–water derivative.

The general form of the μ_{Fe} *versus* temperature curve for (**2**) (assuming the empirical formula $[Fe_3(O)(O_2CPh)_6(py)_2(H_2O)](O_2CPh)\cdot C_6H_5CH_3$ (**2a**) (Fig. 2(a)) is also consistent with antiferromagnetic behaviour. However the value of $\mu_{Fe} = 2.55$ μ_B at 300 K calculated on the basis of that formula is notably lower than the 3.25 μ_B found for the tris-pyridine derivative (**1**) and for other $\{Fe_3(\mu\text{-}O)\}^{7+}$ complexes.[17,18] The value of μ_{Fe} drops to 0.80 μ_B at 5 K. Modelling of the curve using the isosceles triangle model allowed line fitting to be achieved but only with an unacceptably low assumed value of $g = 1.64$ for values of $J = -35.9$ cm^{-1} and $J' = -42.8$ cm^{-1}. The shape of the μ vs. T curve differs in detail from that of (**3**) indicating that (**2**) and (**3**) are dissimilar materials.

The magnetic properties of (**2**) are more comparable with those obtained for a variety of well characterised tetranuclear Fe^{III} compounds[27–29] (Table 3). In fact the microanalytical data obtained for (**2**) also fit well the empirical tetranuclear formula $[Fe_4(O)_2(O_2CPh)_8(py)_2]\cdot 1.5C_6H_5CH_3$ (**2b**). We have explored in detail the fitting of the magnetic data to a tetranuclear, rhomboidal model[30] in which the four Fe atoms designated Fe_1, Fe_2, Fe_3 and Fe_4, run sequentially around the rhombus thus making Fe_2Fe_4 equivalent to the body–body (bb) position in the 'butterfly' $\{Fe_4O_2\}$ model of Hendrickson *et al.*[28] with Fe_1Fe_2, Fe_1Fe_4, Fe_3Fe_2 and Fe_3Fe_4 being the wing–body (wb) interacting atom pairs. The Fe_1Fe_3 wing–wing atoms were assumed not to couple. The spin Hamiltonian employed therefore was:

$$\mathscr{H} = -2\boldsymbol{J}_{12}(\boldsymbol{S}_1\cdot\boldsymbol{S}_2 + \boldsymbol{S}_2\cdot\boldsymbol{S}_3 + \boldsymbol{S}_3\cdot\boldsymbol{S}_4 + \boldsymbol{S}_4\cdot\boldsymbol{S}_1) - 2\boldsymbol{J}_{24}\boldsymbol{S}_2\cdot\boldsymbol{S}_4$$

Table 3 Magnetic moment data for Fe^{III} compounds prepared in this study and other tetranuclear Fe^{III} compounds

Compound	Magnetic moments (μ_{eff} per Fe/μ_B) 300 K	4.5 K
$[Fe_3(O)(O_2CPh)_6(py)_3](NO_3)$ (**1**)	3.25	0.8
Compound (**2**)	2.55[a]	0.70
	2.42[b]	0.66
$[Fe_6(\mu_3\text{-}O)_2(\mu\text{-}OH)_2(O_2CPh)_{12}(py)_2]\cdot 2EtO_2CMe\cdot H_2O$ (**3**)	3.70	1.15
$[Fe_2Zr_2(\mu_3\text{-}O)_2(O_2CPh)_6(OBu^t)_4(py)_2]\cdot 2C_6H_5CH_3$ (**4**)	5.81	1.26[c]
$[Fe_3(O)(O_2CPh)_6(H_2O)_3](O_2CPh)$ [18]	3.39	1.77[d]
$[Fe_4(O)_2(O_2CCH_3)_7(bpy)_2](ClO_4)$ [28]	2.10	0.41[e]
$(Et_4N)[Fe_4(O)_2(O_2CPh)_7(H_2B(pz)_2)_2]$ [29]	2.33	0.16[f]
$[Fe_4(O)_2(BICOH)_2(BICO)_2(O_2CPh)_4]Cl_2$ [27]	2.40	0.4

(bpy) = 2,2′-bipyridyl; $(H_2B(pz)_2)^-$ = dihydrobis(1-pyrazolyl)borate; (BICOH) = bis(*N*-methylimidazol-2-yl)carbinol. [a] Calc. as $[Fe_3(O)(O_2CPh)_6(py)_2(H_2O)](O_2CPh)\cdot C_6H_5CH_3$. [b] Calc. as $[Fe_4(O)_2(O_2CPh)_8(py)_2]\cdot 1.5C_6H_5CH_3$. [c] Measured at 2 K. [d] 20.8 K. [e] 5 K. [f] 6 K.

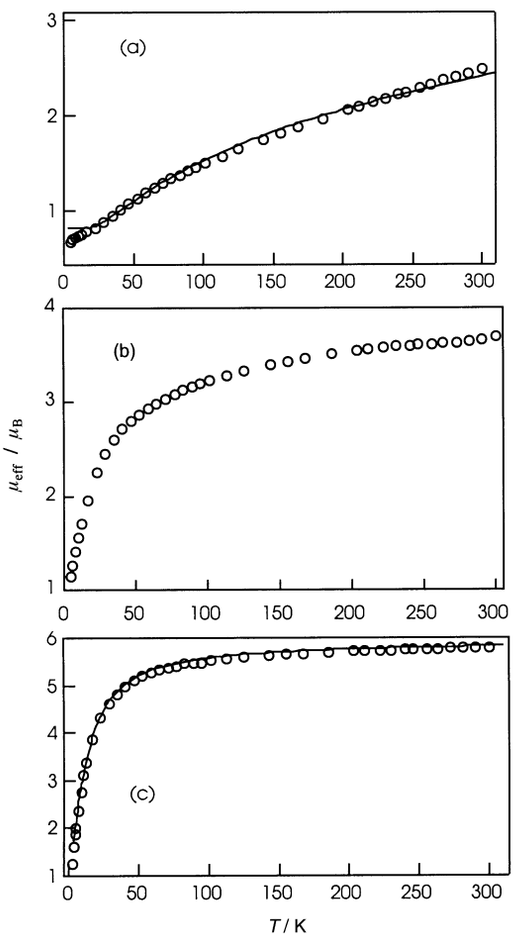

Fig. 2 The variation of magnetic moment, μ_{eff}, per Fe with temperature: (a) compound (**2**) expressed as $[Fe_3(\mu_3\text{-}O)(O_2CPh)_6(py)_2(H_2O)](O_2CPh)$, the solid line represents the best fit obtained by the isosceles triangle model; (b) $[Fe_6(\mu_3\text{-}O)_2(\mu\text{-}OH)_2(O_2CPh)_{12}(py)_2]\cdot 2EtO_2CMe\cdot H_2O$ (**3**); (c) $[Fe_2Zr_2(\mu_3\text{-}O)_2(\mu\text{-}O_2CPh)_6(OBu^t)_4(py)_2]\cdot 2C_6H_6$ (**4**), the solid line shows the best fit using an $S = 5/2$ dimer model.

Inclusion of *n* mole fraction of "monomeric impurity" was required to fit the data and was included in the total susceptibility, χ (per 4Fe cluster):

$$\chi = n\chi_{Fe(S=5/2)} + (1 - n)(\chi_{4Fe} + TIP)$$

$\chi_{Fe(S=5/2)}$ was calculated using the Hamiltonian $\mathscr{H} = g\beta \boldsymbol{H}\cdot \boldsymbol{S}$ (β is the Bohr Magneton; TIP = temperature independent paramagnetism). Since the antiferromagnetic coupling is strong (μ (per 4Fe cluster) = 4.84 μ_B *versus* 11.83 μ_B for four uncoupled

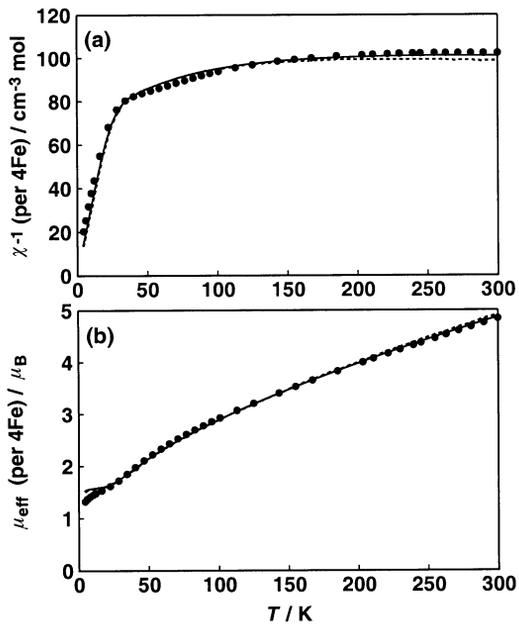

Fig. 3 (a) Plot of χ^{-1} (per 4Fe cluster) *versus* temperature for compound (**2**), the solid line is that calculated using the {tetranuclear $S = 5/2$ + monomer} model with J_{24} (J_{bb}) = +34 cm^{-1}, the dotted line uses $J_{24} = 0$ cm^{-1}, both have J_{12} (J_{wb}) = −38.9 cm^{-1}; (b) equivalent plots of observed and calculated magnetic moment, μ_{eff} per 4Fe cluster, for compound (**2**).

Fe^{III} ions), the $S = 0$ state is populated at low temperature and the Van Vleck susceptibility equation can be used to calculate χ_{4Fe} for the tetramer. The 'high' moment of 1.32 μ_B, per 4Fe cluster, observed at 4.5 K is due to the thermal population of a single $S = 5/2$ state, rather than to a low-lying coupled state of the tetramer, since χ^{-1} *vs.* *T* is linear below 25 K. The tetramer does not contribute to χ in this region. In fitting, the observed and calculated χ values, the *g* values for the tetramer and the $S = 5/2$ species were set at 2.0 and the TIP at 800×10^{-6} cm^3 mol^{-1} (a value also used by Hendrickson *et al.*[28]). A slightly bigger value of *n* than that estimated from the susceptibility values below 16 K, *viz.*, 0.07 or 7%, yielded a good fit to the data over the whole temperature range with some discrepancy below 16 K, probably due to zero-field splitting effects. A very good fit to the data was obtained for a J_{12} value of −38.9 cm^{-1} and incorporation of J_{24} = +34 cm^{-1} gave an improved fit, above 120 K, compared to $J_{24} = 0$ cm^{-1} (Fig. 3). However, this positive value of J_{24} may not be significant since it is known that J_{24} is indeterminate in $\{Fe_4O_2\}$ systems because of spin-frustration.[28] The J_{12} (J_{wb}) value compares well to the value of −45.5 cm^{-1} for $[Fe_4(O)_2(O_2CCH_3)_7(bpy)_2](ClO_4)$[28] and −42 cm^{-1} for $(Et_4N)[Fe_4(O)_2(O_2CPh)_7(H_2B(pz)_2)_2]$[29] suggesting that

Table 4 Mössbauer spectral data for compounds prepared in this study and other selected tetranuclear Fe^{III} compounds (δ values relative to α-Fe at room temperature; figures in parentheses represent two standard deviations)

Compound	Mössbauer parameters				
	δ/mm s^{-1}	ΔE_Q/mm s^{-1}	Γ^a/mm s^{-1}	Area (%)	T/K
$[Fe_3(O)(O_2CPh)_6(py)_3](NO_3)$ (**1**)	0.52(5)	0.63(8)	0.31(1)	100	81
Compound (**2**)	0.52(2)	1.44(2)	0.32(1)	26(5)	81
	0.49(2)	1.11(2)	0.32(1)	24(5)	
	0.53(1)	0.74(1)	0.32(1)	50(10)	
$[Fe_6(\mu_3\text{-}O)_2(\mu\text{-}OH)_2(O_2CPh)_{12}(py)_2]\cdot 2EtO_2CMe\cdot H_2O$ (**3**)	0.54(1)	0.80(1)	0.29(1)	70(4)	81
	0.54(1)	0.52(1)	0.28(1)	30(4)	
$[Fe_2Zr_2(\mu_3\text{-}O)_2(O_2CPh)_6(OBu^t)_4(py)_2]\cdot 2C_6H_6$ (**4**)	0.52(2)	0.74(2)	0.80(2)[b]	100	81
			1.02(2)[c]		
$[Fe_3(O)(O_2CPh)_6(H_2O)_3](O_2CPh)$ [18]	0.51(1)	0.65(1)	0.40(1)	100	5
	0.53	0.45	0.38		78
$[Fe_4(O)_2(O_2CCH_3)_7(bpy)_2](ClO_4)$ [28]			0.40		
	0.457(2)	1.333(3)	0.177(2)		105
			0.178(2)		
	0.487(2)	0.962(4)	0.198(3)		
$[Fe_4(O)_2(O_2CCF_3)_8(H_2O)_6]$ [31]			0.186(3)		
	0.55(1)[d]	1.10	0.33		80
$(Et_4N)[Fe_4(O)_2(O_2CPh)_7(H_2B(pz)_2)_2]$ [29]	0.55(1)[d]	0.45	0.33		
$[Fe_4(O)_2(BICOH)_2(BICO)_2(O_2CPh)_4]Cl_2$ [27]	0.52	1.21			80
	0.5(3)	0.81			4.2

[a] Γ = full width at half-height, lowest velocity line given first when widths not equal. [b] L.H. peak. [c] R.H. peak. [d] Corrected to α-Fe standard from $Na_2[Fe(NO)(CN)_5]$ standard.

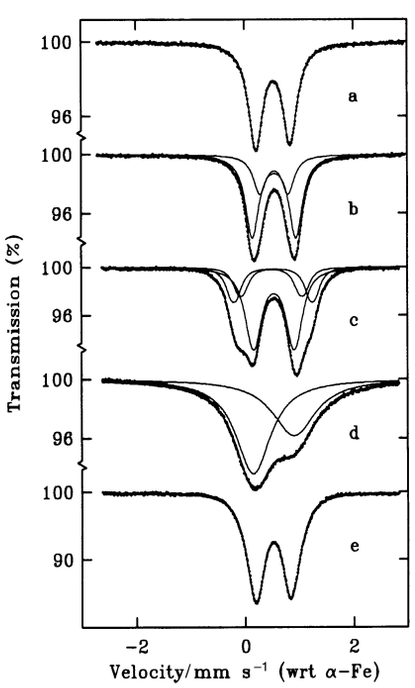

Fig. 4 Mössbauer spectra obtained at 81 K: (a) $[Fe_3(\mu_3\text{-}O)(O_2CPh)_6(py)_3](NO_3)$ (**1**); (b) $[Fe_6(\mu_3\text{-}O)_2(\mu\text{-}OH)_2(O_2CPh)_{12}(py)_2]\cdot 2EtO_2CMe\cdot H_2O$ (**3**); (c) compound (**2**); (d) $[Fe_2Zr_2(\mu_3\text{-}O)_2(\mu\text{-}O_2CPh)_6OBu^t)_4(py)_2]\cdot 2C_6H_6$ (**4**); (e) the spectrum of (**4**) obtained at 5 K. Experimental points are given as dots. Solid lines are the constituent doublet and total lineshape.

(**2**) contains a similar $\{Fe_4O_2\}$ moiety. This is also borne out by the Mössbauer spectral results now described.

The Mössbauer spectra of (**1**) and (**3**) are quite dissimilar to each other and to that of (**2**). Thus $[Fe_3(\mu_3\text{-}O)(O_2CPh)_6(py)_3](NO_3)$ (**1**) displays a single asymmetrical doublet (Fig. 4(a)), the relative intensities of the two lines being 1 : 0.95. The doublet's parameters (Table 4) are quite comparable to those of other symmetrically substituted $Fe_3(\mu\text{-}O)$ "basic" carboxylates.[18] The spectrum of the hexanuclear product (**3**) (Fig. 4(b)) has a symmetrical distribution which is well defined by two unresolved quadrupole doublets having the parameters shown in Table 4. The ratio of their areas is 2 : 1, within error, in agreement with the existence of the two magnetically different Fe^{III} sites demonstrated by the structural study. The "twisted" boat shape of the molecule should nevertheless produce some slight differences in the Mössbauer spectral response of each of the four Fe atoms in the "deck" position and this is reflected in the slight degree of "misfit" to the experimental data, evident in a large scale plot of the spectrum.

The form of the Mössbauer spectrum of (**2**) (Fig. 4(c)) is clearly not that of a simple doublet and, in appearance, is reminiscent of the four peak spectrum reported[31] for $[Fe_4(\mu_3\text{-}O)_2(O_2CCF_3)_8(H_2O)_6]$, which could be modelled by two partially symmetric doublets in line with the planar configuration of the complex.[32] The spectrum of (**2**) can be fitted by three symmetrical doublets with areas close to the ratio 2 : 1 : 1. However, the areas (but not the hyperfine parameters) are very sensitive to the lineshape used, for example Lorentzian or Voigtian. The quoted errors in the areas in Table 4 reflect this lack of orthogonality in the parameters.

Although the Mössbauer spectrum of a structurally characterised, unsymmetrically substituted, $[Fe_3(O)(O_2CR)_6(L)_2(L')]X$ compound such as corresponds to the empirical formula of (**2a**) has not been previously reported, it may be predicted that it should be modelled by two quadrupole doublets whose areas would be in the ratio 2 : 1 in line with the two different Fe^{III} sites expected. The Mössbauer spectra of several $\{Fe_4(\mu_3\text{-}O)_2\}^{8+}$ core compounds have been reported (Table 4) with planar (D_{2h})[27,31] or "butterfly" (C_2)[28,29] symmetries. These spectra have been modelled by two equivalent doublets, as predicted on the basis of two pairs of differently coordinated Fe sites,[28,31] or single doublets,[27,29] apparently depending on the relative Fe–(μ_3-O) bond distances of the two pairs of Fe atoms (body or "wing tip") and not on the steric arrangement of the cluster.[29] Complexes having relatively large differences between the sets of distances appeared most likely to give spectra capable of being fitted by two doublets. While these complexes show isomer shifts (δ) within the range expected for high spin Fe^{III} compounds they also show large quadrupole splitting parameters ($\Delta E_Q > 1$ mm s^{-1}) for either one of the two fitted doublet values or the single doublet (Table 4), and this has been related to a substantial distortion from octahedral symmetry at the Fe^{III} sites.[29] The Fe atoms at the "wing tip" positions have been associated with the larger ΔE_Q values.[29,31] The ΔE_Q values for each of the two doublets of smaller area fitted to the spectrum

of (**2**) are comparable to the larger literature values *i.e.* to "wing tip" Fe sites, while the doublet of larger area has a value comparable to the smaller, "body site" ΔE_Q values. In anticipation of the later discussion in this paper of an Fe_2Zr_2 complex, formed with the aid of (**2**) as an intermediate, which has a "butterfly" configuration with two Fe atoms making up the "body", the single doublet capable of defining the Mössbauer spectrum of that compound has a ΔE_Q of comparable value to that of the larger doublet (50% area) used to define the spectrum of (**2**) as well as the values associated with "body sites" in other Fe_4O_2 compounds. If (**2**) does have a tetranuclear constitution and a rhomboidal form as suggested by the magnetic evidence, an interpretation of its Mössbauer spectrum would require that the "wing tip" Fe sites differ in some way from each other while the "body" sites are equivalent to each other but differ from the "wing tip" sites. A plausible formula and constitution of (**2**), in keeping with the various other known structures, could be $[Fe_4(\mu_3\text{-}O)_2(O_2CPh)_8(py)_2]$ with the four Fe atoms in either planar or "butterfly" array. Six carboxylate residues could link "wing tip" and "body" Fe sites (three per $Fe_3(\mu_3\text{-}O)$ segment) either singly or in pairs, as observed for other $Fe_4(\mu_3\text{-}O)_2$ benzoate compounds.[28,29] Pyridine molecules linked to the "body" Fe atoms would provide for equivalent 6-coordinate Fe at these sites while the "wing tip" Fe atoms could achieve 6-fold coordination in either of two ways. One would involve chelation of one of the remaining carboxylate groups to a "wing tip" site, the other would involve the remaining carboxylate binding as a monodentate ligand with its second oxygen free to bridge to a "wing tip" site on a neighbouring $Fe_4(\mu_3\text{-}O)_2$ molecule. This site could finally achieve 6-fold coordination by receiving another monodentate carboxylate bridge from the second Fe_4 molecule. Compound (**2**) could therefore potentially exist as an Fe_4 dimer with three dissimilar types of Fe sites in the ratio 2 : 1 : 1. A structural study of the material is clearly needed to resolve the matter and must await a superior technique for isolating crystals of suitable quality for an X-ray study. The failure to readily obtain an authentic tris-pyridine derivative from $[Fe_3(O)(O_2CPh)_6(H_2O)_3](O_2CPh)$ is however surprising. Since the stable and structurally characterised derivatives, $[Fe_3(\mu_3\text{-}O)(O_2CPh)_6(py)_3]X$, $X = NO_3$,[16a] ClO_4[16b] were readily prepared by essentially the same route as used in the present study, it is possible that the presence of a benzoate counter ion may influence whether a stable $[Fe_3(O)(O_2CPh)_6(py)_3]^+$ cationic unit can be isolated in the crystal state.

Nevertheless, despite the uncertainty as to its actual constitution, the toluene solubility of (**2**) made it a useful precursor for the synthesis of an Fe–Zr oxo–alkoxo–carboxylato compound as described in the following section.

Isolation of $[Fe_2Zr_2(\mu_3\text{-}O)_2(\mu\text{-}O_2CPh)_6OBu^t)_4(py)_2]$ (4)

Compound (**2**) was initially reacted with $Zr(OR)_4$ (R = Pr^n, Pr^i, Bu^n, Bu^t) in toluene and benzene at room temperature. The Fe^{III} complex was sparingly soluble at room temperature in dry benzene or toluene but began to dissolve when any of the $Zr(OR)_4$ reagents was added to the mixture indicating that a reaction was occuring. In order to achieve full solubility of the Fe compound, it was necessary to add at least three molar equivalents of any of the $Zr(OR)_4$ compounds examined.

Slow evaporation of the solutions obtained from reactions involving $Zr(OR)_4$ (R = Pr^n, Pr^i and Bu^n), failed to deposit crystalline material from any of the solvents tried. Instead, transparent red solids were obtained on eventual evaporation of the solutions to dryness. However, a yellow crystalline product was readily obtained when the branched chain derivative, $Zr(OBu^t)_4$, was used with benzene as solvent. A single crystal X-ray diffraction study established that the compound was a di-benzene solvate of the heterometallic complex

Table 5 Selected bond distances (Å) and angles (°) for $[Fe_2Zr_2(\mu_3\text{-}O)_2(O_2CPh)_6(OBu^t)_4(py)_2]\cdot 2C_6H_6$ (**4**) (estimated standard deviations in parentheses)

Fe(1)–O(1)	1.920(2)	Zr(1)–O(1)	2.09(2)
Fe(1)–O(8)	2.048(2)	Zr(1)–O(3)	1.946(2)
Fe(1)–O(9)	2.063(2)	Zr(1)–O(7)	2.163(2)
Fe(1)–O(17)	2.016(2)	Zr(1)–O(14)	2.163(2)
Fe(1)–N(1)	2.174(2)	Zr(1)–O(18)	2.246(2)
Fe(2)–O(1)	1.954(2)	Zr(2)–O(15)	2.254(2)
Fe(2)–O(16)	2.017(2)		
O(1)–Fe(1)–O(2)	84.30(7)	O(1)–Fe(1)–O(8)	98.46(7)
O(1)–Fe(1)–O(9)	176.46(7)	O(1)–Fe(1)–O(17)	93.44(7)
O(1)–Fe(1)–N(1)	94.41(7)	O(2)–Fe(1)–O(8)	171.66(7)
O(8)–Fe(1)–O(9)	84.27(7)	O(8)–Fe(1)–O(17)	88.23(7)
O(8)–Fe(1)–N(1)	81.23(7)	O(9)–Fe(1)–O(17)	84.37(7)
O(9)–Fe(1)–N(1)	88.21(7)	O(17)–Fe(1)–N(1)	167.67(7)
O(1)–Fe(2)–O(12)	171.17(7)	O(1)–Fe(2)–O(13)	93.47(7)
O(1)–Fe(2)–O(16)	98.01(7)	O(1)–Fe(2)–N(2)	90.50(7)
O(12)–Fe(2)–O(13)	85.78(7)	O(13)–Fe(2)–N(2)	85.09(7)
O(1)–Zr(1)–O(3)	93.44(7)	O(1)–Zr(1)–O(4)	167.70(7)
O(1)–Zr(1)–O(7)	88.35(6)	O(1)–Zr(1)–O(14)	87.62(6)
O(1)–Zr(1)–O(18)	82.25(6)	O(3)–Zr(1)–O(4)	98.86(7)
O(3)–Zr(1)–O(7)	90.26(7)	O(3)–Zr(1)–O(14)	117.97(7)
O(3)–Zr(1)–O(18)	170.88(7)	O(7)–Zr(1)–O(14)	117.97(7)
O(7)–Zr(1)–O(18)	81.62(6)	O(14)–Zr(1)–O(18)	90.95(6)
Fe(1)–O(1)–Fe(2)	95.49(7)	Fe(1)–O(1)–Zr(1)	126.62(8)
Fe(2)–O(1)–Zr(1)	130.43(8)		

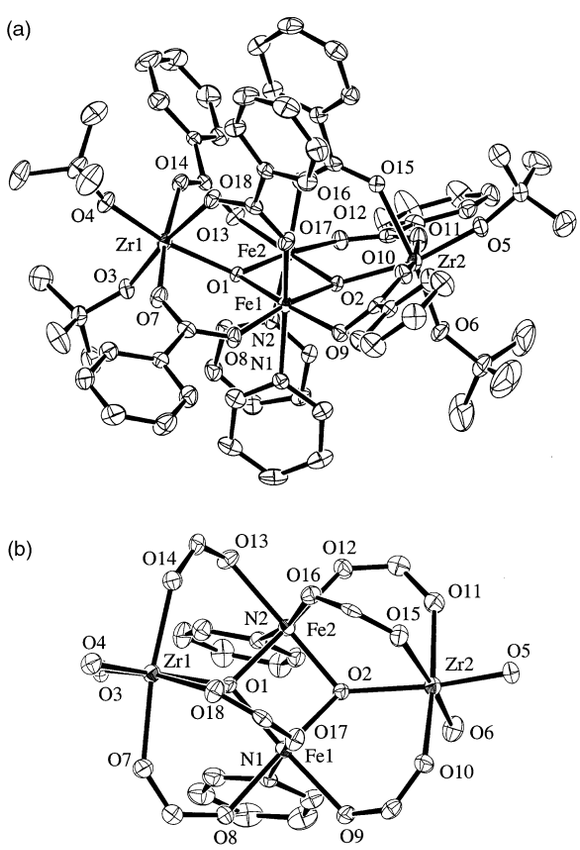

Fig. 5 ORTEP diagrams: (a) $[Fe_2Zr_2(\mu_3\text{-}O)_2(\mu\text{-}O_2CPh)_6(OBu^t)_4(py)_2]\cdot 2C_6H_6$ (**4**); (b) the $\{Fe_2Zr_2(\mu_3\text{-}O)_2\}^{10+}$ skeletal core.

$[Fe_2Zr_2(\mu_3\text{-}O)_2(\mu\text{-}O_2CPh)_6(OBu^t)_4(py)_2]$. An ORTEP diagram of the molecule is presented in Fig. 5(a) with views of the core, including only immediate peripheral ligand attachments in Fig. 5(b).

The only alkoxide moities in the molecule are *tert*-butoxide groups terminally coordinated to each Zr atom. It is an interesting observation that no alkoxide or carboxylate bridging is found between Fe and Zr atoms nor any complete transfer of a carboxylate from Fe to Zr or alkoxide from Zr to Fe. The only

Table 6 Comparisons of average bond distances in $Zr_3(\mu_3\text{-O})$ and $Zr_4(\mu_4\text{-O})$ core complexes

Complex	Zr–(μ_3-O)/Å	Zr–$(OR)_{term}$/Å	Zr–$(OR)_{bridg}$/Å	Zr-$(O_2CR)_{bridg}$/Å
$[Zr_3(\mu_3\text{-O})(OBu^t)_8(O_2CPh)_2]$ (**5**)	2.082	1.928	2.164	2.225
$[Zr_3(\mu_3\text{-O})(OH)_3(O_2CPh)_3(\eta^5\text{-}C_5H_5)_3](O_2CPh)$ [42]	2.071			2.192
$[Zr_3(\mu_3\text{-O})(\mu_3\text{-Cl})(OCH_2Bu^t)_9]$ [40]	2.086	1.929	2.166	
$[Zr_3(\mu_3\text{-O})(OH)(OBu^t)_9]$ [40]	2.101	1.930	2.172	
$\{Na_2[Zr_3(\mu_3\text{-O})(OEt)_{12}]\}_2$ [40]	2.178	1.944	2.107	
$[Zr_4(\mu_4\text{-O})(OPr^i)_{10}(acac)_4]$ [43]	2.16	1.94	2.19	

other Fe–Zr carboxylate derivative to have been characterised, $[FeZr_3(\mu_4\text{-O})(\mu\text{-}OPr^n)_6(OPr^n)_4(acac)_3]$,[7] involving reaction between $Fe(acac)_3$ and $Zr(OPr^n)_4$ resulted in complete transfer of acetylacetonate ions from Fe to Zr. The reaction of (**2**) with $Ti(OR)_4$ also involves such an extreme degree of alkoxide and carboxylate exchange between Fe and Ti centres that separate polynuclear Fe and Ti complexes were formed and Fe–Ti complexes could not be isolated.[33]

Table 1 contains the crystallographic data for the complex with selected bond distances and angles in Table 5. The molecule possesses an $\{Fe_2Zr_2(\mu_3\text{-O})_2\}^{10+}$ core which may be considered as the combination of two $\{Fe_2Zr(\mu_3\text{-O})\}^{8+}$ triangular units sharing a common Fe–Fe edge. The four metal atoms are disposed in a "butterfly" type arrangement with the two Fe atoms forming the "body". The dihedral angle between the planes Zr(1)–Fe(1)–Fe(2) and Zr(2)–Fe(l)–Fe(2) is 152.5°. The μ_3-oxo groups are displaced by *ca*. 0.3 Å from their respective Fe_2Zr planes. The μ_3-oxo linking of metal atoms in the $\{Fe_2Zr_2(\mu_3\text{-O})_2\}^{10+}$ core is reinforced through six bridging benzoate moieties between Fe and Zr centres arranged either singly or in pairs. The pyridine ligands coordinated to the Fe^{III} atoms are directed "downwards", away from the Fe_2Zr planes.

Each Fe and Zr atom has approximate octahedral stereochemistry, the various O–Fe(1)–O angles lying in the range 84.27–99.49° with the O–Zr(1)–O angular range being 82.25–98.86°. The Fe–(μ_3-O) distances are longer when a single carboxylate bridge links that Fe atom to a neighbouring Zr than when two such carboxylate bridges are present, *viz.* Fe(1)–O(1), 1.920(2) Å, Fe(1)–O(8), 2.048(2) Å. Nevertheless, both distances are notably shorter than the Fe–(μ_4-O) length (2.124 Å) in $[FeZr_3(\mu_4\text{-O})(OC_3H_7)_{10}(acac)_3]$.[7] Both types of Fe–($\mu_3$-O) distances are longer than generally reported for Fe_3–(μ_3-O) compounds (*ca*. 1.90 Å[10,23,34]). Overall the Fe–O bond lengths and Fe–O–Fe angles of the Fe_2Zr_2 complex are similar to the Fe_{body}–(μ_3-O) distances and Fe_{body}–O–Fe_{body} angles found in "butterfly" and planar type $Fe_4(\mu_3\text{-O})_2$ compounds as defined in the analyses by Gorun and Lippard[27] and Hendrickson *et al*.[28] Zr–(μ_3-O) distances and angles are comparable with the range of such bond lengths found in other Zr species containing μ-oxo groups (Table 6).

Magnetism and Mössbauer spectrum of (4)

The magnetic susceptibility of $[Fe_2Zr_2(\mu_3\text{-O})_2(\mu\text{-}O_2CPh)_6(OBu^t)_4(py)_2]$ has been measured from 2 to 300 K at a field strength of 1 Tesla. Fig. 2(c) shows the temperature dependence of the effective magnetic moment per Fe, for the complex. The moment of 5.81 μ_B at 300 K is slightly smaller than the 5.92 μ_B appropriate for a mononuclear, high-spin d^5 Fe^{III} complex and the value decreases very gradually between 300 and 100 K, reaching *ca*. 5.60 μ_B at 100 K, before decreasing more rapidly with reduction in temperature to 1.26 μ_B per Fe at 2 K. This overall type of magnetic behaviour is consistent with the presence of weak antiferromagnetic coupling between the two Fe^{III} sites resulting in a slightly reduced magnetic moment for the complex at 300 K. The coupling of Fe^{III} ions presumably occurs *via* the centrally located μ_3-oxo groups bridging the two iron sites. The system may be viewed essentially as an isolated $\{Fe_2O_2\}$ system. An Fe_2 dimer model[25,26] having a spin exchange Hamiltonian of $-2J(\boldsymbol{S}_1\cdot\boldsymbol{S}_2)$ where $\boldsymbol{S}_1 = \boldsymbol{S}_2 = 5/2$, was used to analyse the experimental susceptibility data, with the best fit yielding the parameters $J = -1.42$ cm^{-1} for $g = 2.01$ with a paramagnetic impurity calculated to be *ca*. 1.1%. The very weak nature of the coupling between Fe^{III} atoms in this complex is perhaps surprising, since compounds containing Fe_2O_2 bridges, including $\{Fe_4(\mu_3\text{-O})_2\}^{8+}$ species, generally exhibit relatively strong antiferromagnetic coupling.[35,36] Detailed analysis of the magnetic interactions in $[Fe_4(\mu_3\text{-O})_2(O_2CMe)_7(bpy)_2](ClO_4)$[28] however, indicated that the strongest pairwise interaction for this complex occurred between one wing-tip ion and one of the Fe ions located on the "body" of the molecule, with Fe–O–Fe ≈ 127°. Modelling of the magnetic susceptibility of this compound was found to be surprisingly insensitive to changes in the Fe_{body}–Fe_{body} interaction (Fe–O–Fe ≈ 95°). The J_{bb} value for $[Fe_4(\mu_3\text{-O})_2(O_2CMe)_7(bpy)_2](ClO_4)$ was finally assigned at -8.9 cm^{-1} indicating a relatively weak antiferromagnetic interaction. Similarly, small J values were deduced for the Fe_2O_2 fragment in an $[Fe_2Cr_2(\mu_3\text{-O})_2]^{8+}$ cluster[37] and in an $[Fe_2O_2]^{2+}$ "diamond" core.[38] The present $[Fe^{III}_2(OZr)_2]$ core can also be regarded as being analogous to μ-alkoxo species $[Fe^{III}_2(OR)_2]$ for which J values are also generally small and sometimes close to zero.[39]

The zero-field Mössbauer spectrum of a bulk sample of (**4**) measured at 5 K shows a single doublet (Fig. 4(e)) which can be fitted with an asymmetric doublet having the parameters shown in Table 4. The ratio of the lines is 1 : 0.95 and a Voigt lineshape gave a much better fit than the Lorentzian one. The spectrum is in line with the existence of only one type of Fe^{III} site as defined by the structure. The ΔE_Q value is comparable with the smaller of the values obtained in the fitting of the spectrum of (**2**) and led, in the hypothetical structure suggested for that compound, to coordinated pyridines being located at the "body" Fe sites. The spectrum at 81 K shows a major change in shape (Fig. 4(d)), the reason for which is not clear although it is considered to have an electronic and/or relaxation origin and not be due to any crystallographic reorganisation. The data at 81 K can be fitted as two single Lorentzian lines, with areas in the ratio 1 : 0.8 from which derive the parameters listed in Table 4.

Isolation of a Zr oxo–alkoxy–carboxylate compound (5)

The reaction of (**2**) with a large excess (six molar equivalents) of $Zr(OBu^t)_4$ in benzene allowed full dissolution of the Fe^{III} starting material on stirring at room temperature. As for the reactions employing only one, two or three equivalents of the alkoxide, slow evaporation of this solution resulted in the deposition of crystals. While microanalysis and microprobe examination of the bulk of the crystalline material showed it to be predominantly $[Fe_2Zr_2O_2(O_2CPh)_6(OBu^t)_4(py)_2]$, a single, light-yellow coloured crystal which had grown fortuitously away from the bulk of the crystalline mass, was removed from the wall of the flask, and used for a single crystal X-ray diffraction study. The material was characterised as a new trinuclear Zr oxo–alkoxy–carboxylate complex, $[Zr_3(\mu_3\text{-O})(OBu^t)_8(O_2CPh)_2]$ (**5**). Crystallographic data and selected bond distances and angles are contained in Tables 1 and 7, respectively. An ORTEP diagram of the complex is shown in Fig. 6. The presence of carboxylate moieties in the structure of the Zr trimer shows that exchange reactions have taken place between

Table 7 Selected bond distances (Å) and angles (°) for $[Zr_3(\mu_3\text{-}O)(\mu\text{-}OBu^t)_2(OBu^t)_6(\mu\text{-}O_2CPh)_2]$ (**5**) (estimated standard deviations in parentheses)

Zr(1)–O(1)	1.998(2)	Zr(1)–O(2)	2.125(2)
Zr(1)–O(4)	1.909(2)	Zr(1)–O(5)	1.929(2)
Zr(1)–O(10)	2.165(2)	Zr(2)–O(1)	2.111(2)
Zr(2)–O(6)	1.934(2)	Zr(2)–O(7)	1.929(2)
Zr(2)–O(11)	2.190(2)	Zr(2)–O(12)	2.284(2)
Zr(3)–O(1)	2.166(2)	Zr(3)–O(8)	1.916(2)
Zr(3)–O(9)	1.947(2)	Zr(3)–O(13)	2.221(2)
O(1)–Zr(1)–O(2)	77.12(6)	O(1)–Zr(1)–O(4)	117.60(7)
O(1)–Zr(1)–O(5)	126.60(7)	O(1)–Zr(1)–O(10)	86.60(7)
O(2)–Zr(1)–O(4)	102.54(7)	O(2)–Zr(1)–O(5)	97.71(7)
O(2)–Zr(1)–O(10)	162.77(7)	O(4)–Zr(1)–O(5)	115.40(8)
O(4)–Zr(1)–O(10)	89.89(7)	O(1)–Zr(2)–O(3)	75.23(6)
O(1)–Zr(2)–O(6)	161.05(6)	O(1)–Zr(2)–O(7)	98.69(7)
O(1)–Zr(2)–O(11)	85.97(6)	O(1)–Zr(2)–O(12)	79.14(6)
O(3)–Zr(2)–O(6)	105.49(7)	O(3)–Zr(2)–O(7)	97.48(7)
O(3)–Zr(2)–O(11)	160.84(6)	O(3)–Zr(2)–O(12)	87.34(6)
O(6)–Zr(2)–O(7)	99.95(7)	O(6)–Zr(2)–O(11)	91.07(7)
O(6)–Zr(2)–O(12)	81.98(6)	O(7)–Zr(2)–O(11)	88.87(7)
O(7)–Zr(2)–O(12)	174.07(7)	O(11)–Zr(2)–O(12)	85.48(6)
O(1)–Zr(3)–O(2)	72.13(6)	O(2)–Zr(3)–O(3)	144.70(6)
O(2)–Zr(3)–O(13)	83.59(6)	O(3)–Zr(3)–O(8)	97.61(7)
O(3)–Zr(3)–O(9)	105.69(7)		
Zr(1)–O(1)–Zr(2)	140.09(9)	Zr(1)–O(1)–Zr(3)	108.13(7)
Zr(2)–O(1)–Zr(3)	105.90(7)		

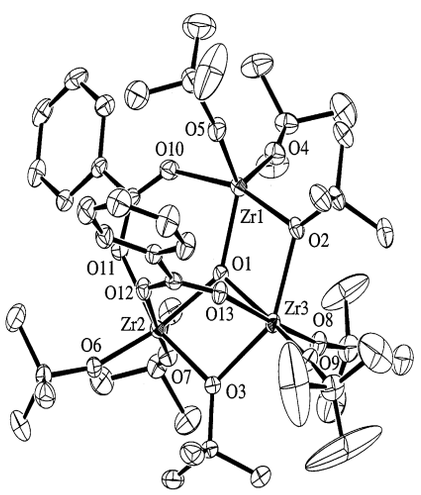

Fig. 6 ORTEP diagram of $[Zr_3(\mu_3\text{-}O)(\mu\text{-}O_2CPh)_2(\mu\text{-}OBu^t)_2(OBu^t)_6]$ (**5**).

the $Zr(OBu^t)_4$ reagent and the initial Fe^{III} carboxylate although the results of such an exchange failed to extend to the constitution of the Fe–Zr complex isolated.

A $\{Zr_3(\mu_3\text{-}O)\}^{10+}$ unit forms the core of the molecule with pairs of terminally bonded alkoxo groups attached to each metal site. A carboxylato and alkoxo group together bridge Zr(2) and Zr(3) while a single carboxylate group bridges Zr(1) and Zr(2) and an alkoxide, Zr(1) and Zr(3). These ligand dispositions lead to 5-coordinate Zr(1) and 6-coordinate Zr(2) and Zr(3). The differing stereochemistries of the Zr atoms and particularly the bridging of Zr(1) and Zr(2) by the two oxygen atoms of a carboxylate group compared with a single OBu^t between Zr(1) and Zr(3) cause the Zr_3O unit to be considerably distorted from a trigonal $Zr_3(\mu_3\text{-}O)$ array. Nevertheless the sum of the individual angles about O(1) totals 354.1° with the μ_3-oxygen atom deviating from the metal atom plane by 0.28 Å. These stereochemical and bridging factors also combine to cause the 5-coordinate Zr bond Zr(1)–(μ_3-O), to be noticeably shorter than either of the 6-coordinate Zr–(μ_3-O) links. The formation of alkoxide bridges between two and even three Zr atoms has been observed previously in $[Zr_3(\mu_3\text{-}O)(\mu\text{-}OH)(\mu\text{-}OBu^t)_2(\mu_3\text{-}OBu^t)(OBu^t)_6]$[40] and $\{Na_2[Zr_3(\mu_3\text{-}O)(\mu OEt)_7(\mu_3\text{-}OEt)_2(OEt)_3]\}_2$.[40] $Zr(OBu^t)_4$, and other *tertiary* alkoxide derivatives of Zr have been reported to be monomeric[41] in solution, inferring that alkoxide bridges cannot form because of steric hindrance effects. Such steric forces could be weakened in the crystal state by the shared binding of the small μ_3-oxo ligand between several Zr atoms leading to easier bond formation with alkoxide oxygen atoms. The additional presence of carboxylato groups with their widely spaced donor oxygens as in the present Zr complex would be expected to further aid in bridge formation by alkoxide ligands by allowing a bridging alkoxide group to be more easily accommodated. The strain experienced by the alkoxide groups in bridging the metal atoms in the complex nevertheless shows in the angular distortions about each metal atom. Thus, the *cis*-O–Zr–O angles around the 6-coordinate metal centres Zr(2) and Zr(3), range between *ca*. 72° and 106° with *trans* angles of *ca*. 145°. Similarly the 5-coordinate centre Zr(1), has considerably distorted trigonal bipyramidal stereochemistry, with angles ranging from *ca*. 77° to 163°. The observation that the oxo group of the $Zr_3(\mu_3\text{-}O)$ core is only 0.28 Å from the Zr_3 plane indicates that the bonding requirements of the μ_3-oxo group take precedence over the stereochemical needs of the other ligands surrounding the metal centres since location of the oxo group further from the Zr_3 plane would help alleviate ligand strain about the three Zr atoms.

There are a number of other $Zr_3(\mu_3\text{-}O)$ species known having the central core units $\{Zr_3(\mu_3\text{-}O)\}^{10+}$ and containing either carboxylate or alkoxide groups together with other ligands (Table 6). The complex described here represents the first structurally characterised Zr–oxo species having both alkoxide and carboxylate moieties within the same molecule. Although the lengths of comparable bonds in each separate class of molecule are similar, there is a greater variability in bond distances in the present Zr_3 compound presumably arising from the asymmetric distribution of bridging ligands.

Acknowledgements

The authors wish to acknowledge support of this research by grants from the Australian Research Council (to K. S. M.; L. S. and B. O. W.; J. D. C.), the award of an Australian Post graduate Research Award (to C. M. K.), an APRA (Industry) and a Monash Research Scholarship (to P. S. A.) and financial and scientific support from Sustainable Technologies Australia Limited. Mr K. J. Berry is thanked for his extensive input into calculations of magnetism.

References

1 K. G. Caulton and L. G. Hubert-Pfalzgraf, *Chem. Rev.*, 1990, **90**, 969.
2 C. D. Chandler, C. Roger and M. J. Hampden-Smith, *Chem. Rev.*, 1993, **93**, 1205.
3 P. Berthet, J. Berthon and A. Revcolevschi, *Physica B* (*Amsterdam*), 1989, **158**, 506.
4 I. B. Inwang, F. Chyad and I. J. McColm, *J. Mater. Chem.*, 1995, **5**, 1209.
5 M. V. Tsodikov, O. V. Bukhtenko, O. G. Ellert, V. M. Shcherbakov and D. I. Kochubey, *J. Mater. Sci.*, 1995, **30**, 1087.
6 R. Schmid, A. Mosset and J. Galy, *C. R. Acad. Sci.*, *Ser II*, 1990, **311**, 1167.
7 R. Schmid, H. Ahamdane and A. Mosset, *Inorg. Chim. Acta*, 1991, **190**, 237.
8 A. Shah, A. Singh and R. C. Mehrotra, *Inorg Chim. Acta*, 1988, **141**, 289; *Indian J. Chem.*, *Sect. A*, 1987, **26**, 485.
9 A. Leaustic, F. Babonneau and J. Livage, *Chem. Mater.*, 1989, **1**, 248.
10 R. D. Cannon and R. P. White, *Prog. Inorg. Chem.*, 1988, **36**, 195.
11 A. Trzeciak, T. Szymanska-Buzar and J. J. Ziolkowski, *Polish J. Chem.*, 1979, **53**, 981.
12 K. L. Taft, C. D. Delfs, G. C. Papaefthymiou, S. Foner, D. Gatteschi and S. J. Lippard, *J. Am. Chem. Soc.*, 1994, **116**, 823.
13 C. Benelli, S. Parsons, G. A. Solan and R. E. P. Winpenny, *Angew. Chem.*, *Int. Ed. Engl.*, 1996, **35**, 1825.

14 P. Ammala, J. D. Cashion, C. M. Kepert, B. Moubaraki, K. S. Murray, L. Spiccia and B. O. West, *Angew. Chem.*, *Int. Ed.*, 2000, **39**, 1688.
15 R. F. Weinland and A. Herz, *Chem. Ber.*, 1912, **45**, 2662.
16 (*a*) A. M. Bond, R. J. H. Clark, D. G. Humphrey, P. Panayiotopoulos, B. W. Skelton and A. H. White, *J. Chem. Soc.*, *Dalton Trans.*, 1998, 1845; (*b*) F. E. Sowrey, C. Tilford, S. Wocadlo, C. E. Anson, A. K. Powell, S. M. Bennington, W. Montfrooij, U. A. Jayasooriya and R. D. Cannon, *J. Chem. Soc.*, *Dalton Trans.*, 2001, 862.
17 A. Earnshaw, B. N. Figgis and J. Lewis, *J. Chem. Soc. A*, 1966, 1656.
18 G. J. Long, W. T. Robinson, W. P. Tappmeyer and D. L. Bridges, *J. Chem. Soc.*, *Dalton Trans.*, 1973, 573.
19 teXsan, Crystal Structure Analysis Package, Molecular Structure Corporation, Wisconsin, MA, 1985 and 1992.
20 D. T. Cromer and J. T. Waber, *International Tables for X-ray Crystallography*, the Kynoch Press, Birmingham, 1994, vol. IV, Table 2.2A.
21 S. Uemura, A. Spencer and G. Wilkinson, *J. Chem. Soc.*, *Dalton Trans.*, 1973, 2565; R. Wu, M. Poyraz, F. E. Sowrey, C. E. Anson, S. Wocadlo, A. K. Powell, U. A. Jayasooriya, R. D. Cannon, T. Nakamoto, M. Katada and H. Sano, *Inorg. Chem.*, 1998, **37**, 1913; M. K. Johnson, D. B. Powell and R. D. Cannon, *Spectrochim. Acta*, *Part A*, 1981, **37**, 995; A. B. Blake, A. Yavari, W. E. Hatfield and C. N. Sethulekshmi, *J. Chem. Soc.*, *Dalton Trans.*, 1985, 2509.
22 J. B. Vincent, H.-R. Chang, K. Folting, J. C. Huffman, G. Christou and D. N. Hendrickson, *J. Am. Chem. Soc.*, 1987, **109**, 5703. J. Ribas, B. Albela, H. Stoeckli-Evans and G. Christou, *Inorg. Chem.*, 1997, **36**, 2352; X. Hao, L. Jin-Yu, L. Q. X. Zheng, Y. Xiao-Zeng and Y. Kai-Bei, *Struct. Chem.*, 1994, **13**, 272.
23 V. M. Lynch, J. W. Sibert, J. L. Sessler and B. E. Davis, *Acta Crystallogr.*, *Sect. C*, 1991, **47**, 866.
24 W. Micklitz and S. J. Lippard, *Inorg. Chem.*, 1988, **27**, 3067.
25 F. E. Mabbs and D. J. Machin, *Magnetism and Transition Metal Complexes*, Chapman and Hall, London, 1973, pp. 211–215.
26 O. Kahn, *Molecular Magnetism*, VCH, New York, 1993, pp. 195–197.
27 S. M. Gorun and S. J. Lippard, *Inorg. Chem.*, 1988, **27**, 149.
28 J. K. McCusker, J. B. Vincent, E. A. Schmitt, M. L. Mino, K. Shin, D. K. Coggin, P. M. Hagen, J. C. Huffman, G. Christou and D. N. Hendrickson, *J. Am. Chem. Soc.*, 1991, **113**, 3012.
29 W. H. Armstrong, M. E. Roth and S. J. Lippard, *J. Am. Chem. Soc.*, 1987, **109**, 6318.
30 K. S. Murray, *Adv. Inorg. Chem.*, 1995, **43**, 261.
31 R. A. Stukan, V. I. Ponomarev, V. P. Nifontov, K. I. Turté and L. O. Atovmyan, *J. Struct. Chem.* (*Engl. Transl.*), 1985, **26**, 197.
32 V. I. Ponomarev, L. O. Atovmyan, S. A. Bobkova and K. I. Turté, *Dokl. Phys. Chem.* (*Transl. of Dokl. Akad. Nauk*), 1984, **274**, 64.
33 P. S. Ammala, L. Spiccia, A. M. van den Bergen and B. O. West, unpublished observations.
34 A. B. Blake and L. R. Fraser, *J. Chem. Soc.*, *Dalton Trans.*, 1975, 193; D. Fu, G. Wang, W. Tang and K. Yu, *Polyhedron*, 1993, **12**, 2459.
35 D. M. Kurtz, Jr., *Chem. Rev.*, 1990, **90**, 585.
36 R. N. Mukherjee, T. D. P. Stack and R. H. Holm, *J. Am. Chem. Soc.*, 1988, **110**, 1850.
37 P. Chaudhuri, M. Winter, P. Fleischhauer, W. Haase, U. Flörke and H.-J. Haupt, *J. Chem. Soc.*, *Chem. Commun.*, 1993, 566.
38 H.-F. Hsu, Y. Dong, L. Shu, V. G. Young, Jr. and L. Que, Jr., *J. Am. Chem. Soc.*, 1999, **121**, 5230.
39 G. D. Fallon, A. Markiewicz, K. S. Murray and T. Quach, *J. Chem. Soc.*, *Chem. Commun.*, 1991, 198.
40 W. J. Evans, M. A. Ansari and J. W. Ziller, *Polyhedron*, 1998, **17**, 869.
41 D. C. Bradley, R. C. Mehrotra and W. Wardlaw, *J. Chem. Soc.*, 1952, 2027.
42 U. Thewalt, K. Doppert and W. Lasser, *J. Organomet. Chem.*, 1986, **308**, 303.
43 P. Toledano, M. In and C. Sanchez, *C. R. Acad. Sci.*, *Ser. II*, 1990, **311**, 1161.
44 C. K. Johnson, ORTEP, Report ORNL-5138, Oak Ridge National Laboratory, Oak Ridge, TN, 1976.